

THE BURST FROM SNI987a<sup>†</sup>

Adam Burrows

Departments of Physics and Astronomy, University of Arizona  
Tucson, Arizona 85721, USA

## ABSTRACT

The results of a series of general relativistic stellar evolution calculations of the first 20 seconds in the lives of young neutron stars born in Type II supernovae are presented. For each of these models, the theoretical neutrino burst signatures of SNI987a in both the Kamiokande II and IMB water Cherenkov detectors are calculated. The results are compared to the actual Kamiokande II and IMB SNI987a neutrino data to test the general theory of such bursts and to determine the nature of the residue that now resides inside the LMC supernova. It is concluded that the new neutron star in the LMC has a baryon mass between 1.2 and 1.7  $M_{\odot}$  and a best-fit gravitational mass between 1.3 and 1.5  $M_{\odot}$ . The best-fit total energy lost after 20 seconds is  $\sim 2.0\text{--}2.5 \times 10^{53} (D/50 \text{ kpc})^2$  ergs.

In addition, using all the SNI987a neutrino burst events culled by the Kamiokande II detector and a realistic underlying neutrino source model and spectrum, we have performed a series of Monte Carlo calculations to obtain upper limits with confidence levels for the mass of the electron neutrino ( $m_{\nu_e}$ ). With conservative assumptions, the upper limits are 14 eV (90%), 16 eV (95%), and 19 eV (99%). These limits are inconsistent with the *lower* limit quoted by the ITEP collaboration and are lower than all the extant upper limits from tritium decay experiments.

## I. NEUTRINO EMISSION FROM SUPERNOVAE

With the advent of SNI987a in the Large Magellanic Cloud (LMC)<sup>1)</sup> and the detection of the neutrino burst from its core collapse,<sup>2,3)</sup> the supernova community has been animated as never before. SNI987a has already revealed a wealth of fascinating and unexpected phenomena and will be scrutinized across the electromagnetic spectrum for many years to come. As it evolves through successive stages in a supernova explosion never before witnessed with the clarity this supernova's proximity now allows, the prodigious number of its "firsts" is sure to grow.

However, the crowning first associated with the LMC supernova must be the independent epochal detections by both the IMB and the Kamiokande II (KII) collaborations of the neutrino burst from its core. For the first time, we have penetrated the otherwise opaque supernova ejectum and glimpsed at the violent convulsions that attend stellar collapse. The neutrino emissions are the only good signature of core physics, and these detections provide us with the first definitive tests of the basic theory connecting stellar death, supernovae, and neutron star birth.<sup>4)</sup>

Briefly, the white dwarf-like core ( $\sim 1.5 M_{\odot}$ ) of a star whose main sequence mass exceeds  $\sim 8 M_{\odot}$  and whose thermonuclear life lasts  $\sim 10^7$  years collapses within a second to a protoneutron star, whose subsequent transformation into a neutron star proper takes seconds. The shock wave associated with the seconds after collapse travels from the core to the stellar surface in between an hour and a day and disassembles the star in an explosion that lasts months to years. Though  $\sim 10^{49}$  ergs is radiated in supernova light and the kinetic energy of the supernova ejectum is  $\sim 10^{51}$  ergs, more than  $10^{53}$  ergs, or 0.1 to  $0.2 M_{\odot}$ , is liberated in the neutrino burst that simultaneously announces the massive star's death, the neutron star's birth, and the supernova explosion itself. It was such a burst that was detected on Feb. 23.316 (UT) 1987.

It is not the purpose of this paper to perform on the precious KII and IMB numbers the standard maximum-likelihood and Monte Carlo statistical tests to extract the basic parameters of "collapse." A host of workers have already closely scrutinized these columns.<sup>5-11)</sup> Rather, we present the luminosity and temperature behavior of a family of residues with different masses, degrees of post-bounce accretion, etc. Furthermore, the integrated number of events versus time expected in KII and IMB is calculated and plotted for each model for direct comparison with the corresponding actual accumulations. However, a summary of some of the simple conclusions derived with fake models is illuminating and will be presented here without corroboration.

The large angles of the events with respect to the LMC imply that most were not  $\nu$ - $e^-$  scatterings, which are quite forward-peaked (small angle), but that most were indeed  $\bar{\nu}_e$  absorptions. Positron emission following  $\bar{\nu}_e$  absorption in the process,  $\bar{\nu}_e + p \rightarrow n + e^+$ , is almost isotropic. The  $\bar{\nu}_e$  absorption cross section is  $\sim 100$  times the  $\nu_e$ - $e^-$  scattering cross section. However, the IMB data, in particular, show a marked preference for the forward hemisphere that may well be a statistical fluke, but is as yet unexplained.<sup>12,13)</sup> Nevertheless, it seems that

most, if not all, of the events were  $\bar{\nu}_e$  absorptions. The best inferred average source temperature is 3.0-5.0 MeV. There is a slight indication from the data that the source is actually cooling, as one would expect. The late-time events are all lower in energy. The shorter duration of the IMB signal (5.58 seconds) with respect to the KII signal (12.44 seconds) also suggests that the source is cooling, since a given decay in temperature implies an even more rapid decay in the high energy tail of a thermal, or near-thermal, spectrum. The high energy threshold of the IMB detector ( $\sim$ 19 MeV) makes it much more sensitive to this tail than the KII detector with its lower threshold ( $\sim$ 7 MeV) and, hence, one would expect the IMB signal to turn off sooner, as it did.

The evolution of the signal can be fit reasonably well, not by a single exponential, but by two exponentials, one after the other, with  $\tau$ 's of  $\leq$ 1.0 seconds and  $\sim$ 4.0 seconds, respectively. In other words, two phases, an early short one and a later long one, seem indicated. These timescales of seconds are comfortably consistent with the standard model. No neutrino mass, source pulsing, or neutrino oscillations are necessary to explain the data, though none of these exotica are absolutely eliminated. Early ( $t < 0.5$  s)  $\bar{\nu}_e$  luminosities of  $\sim$ 4x10<sup>52</sup> ergs/s (with wide error bars) and later (seconds)  $\bar{\nu}_e$  luminosities of 10<sup>51</sup> ergs/s can, with some trepidation, be derived. These luminosities and the inferred temperatures can be used to obtain radii between 10 and 50 kilometers. There is a slight indication that the radius decreased from the higher value to 10-20 kilometers within the first second. These radii are gratifyingly near those always quoted for neutron stars, and near those for nothing else. The total  $\bar{\nu}_e$  energy radiated is  $\sim$ 3-5x10<sup>52</sup> ergs. If we multiply by 6 to approximately account for the other five neutrino species, a total neutron star binding energy of 2-3x10<sup>53</sup> ergs is derived. This is our first "direct" measurement of a neutron star's binding energy and it is surprisingly close to what was expected.

The generic thermal behavior of the models generated in this new series of simulations is depicted in Figure 1, in which models 59 and 62 (solid lines) serve as representatives of this work, and the results of others<sup>14-17)</sup> are superposed for comparison. Model B11 is from BL, in which the  $\bar{\nu}_e$  opacity was set equal to that for  $\nu_e$ 's. The hatched region highlights the temperature range, 3.0-5.0 MeV, within which the best-fit  $\bar{\nu}_e$  temperature from the KII and IMB data resides. We see that, whereas models 59 and 62, as representatives of the new series, fit comfortably within the hatched region, model B11 is a little too cold. Model BR,<sup>14)</sup> which was carried out for only the first 1.2 seconds, is very similar to models 59 and 62 during that interval, as are models MWS,<sup>15)</sup> M,<sup>16)</sup> and MW.<sup>17)</sup> Curiously, model MWS shows a rapid rise at  $\sim$ 1.0 second to a temperature of  $\sim$ 7.5 MeV. However, the newest Livermore model (MW), the latest in the sequence MWS+M+MW, fits the data reasonably well.

The primary effect of accretion is to maintain higher luminosities longer. Figure 2 depicts the evolution of the antineutrino luminosity versus time for many of the stiff EOS models (52-57, 72). With little or no accretion (models 52-54), the evolution breaks up into two phases. The early fast phase lasts  $\sim$ 500 milliseconds and involves the collapse and

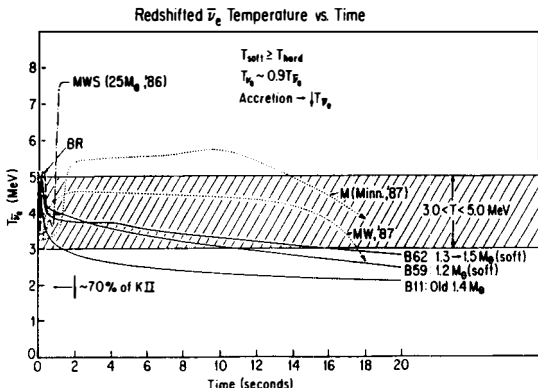


Fig. 1. Redshifted antineutrino temperature  $T_{\bar{\nu}_e}$  in MeV versus time in seconds for selected models from this series of calculations (BII, B59, B62) and those of others before the appearance of SN2087a (Mayle et al. 1987, MWS) and after (Bruenn 1987, BR; Mayle 1987, M; Mayle and Wilson 1987, MW). The time at which 70% of the KII signal has been recorded is marked in the lower left. The  $T_{\bar{\nu}_e}$  evolutions of the other models of this series are similar to those (Bxx) depicted here.

compression of the outer mantle as it cools and neutronizes (BL). During this phase, the antineutrino luminosity is close to  $10^{52}$  ergs/s. Early on ( $< 100$  milliseconds), the neutrinospheres sink in radius from 50-100 kilometers to  $\sim 10$  kilometers, though they move out in mass. The gravitational energy change of the compression is radiated in a standard Kelvin-Helmholtz fashion. As the outer mantle cooling phase subsides, it blends into the long-term diffusive cooling phase of the inner core. The luminosity of the  $\bar{\nu}_e$ 's is then near  $10^{51}$  ergs/s.

The cumulative number of  $\bar{\nu}_e$  events versus time expected in either KII or IMB are plotted in the Figures 3-4. The model parameters and total energy ( $E_T$ ) radiated after 20 seconds are superposed on the graphs for quick reference.  $\dot{M}_0$  is the initial baryon mass accretion rate, and  $\tau$  is the time constant of its decay. The intrinsic source signal strength, the total number of  $\bar{\nu}_e$  events per kilotonne of water at 1 kpc in a perfect detector, is  $\sim (1.6 \pm 0.4) \times 10^4$ . This measure of burst strength is useful for back-of-the-envelope calculations concerning detectors of arbitrary size and future collapses at arbitrary distances.

Figures 3-4 depict the signal expectations for the realistic models with different baryon masses and accretion regimes. They collectively indicate that the general theory presented here for "supernova" neutrinos is quite good. The model grid seems to tightly envelope the observations for both KII and IMB.

Models 52, 53, 57, 69, and 72 seem eliminated as either too weak or too strong. Final baryon masses smaller than  $1.2 M_{\odot}$  or larger than  $1.7 M_{\odot}$  do not fit the data. This leaves models 54-56 as the best fits. Their final baryon masses are in the  $1.4-1.6 M_{\odot}$  range,

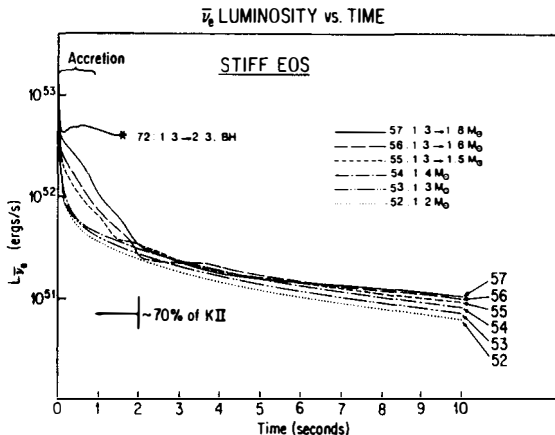


Fig. 2. Redshifted antineutrino luminosity ( $L_{\bar{\nu}_e}$ ) in units of  $10^{51}$  ergs/s versus time in seconds for the stiff EOS models 52-57 and 72. Only the first 10 seconds of the life of the protoneutron star are covered.

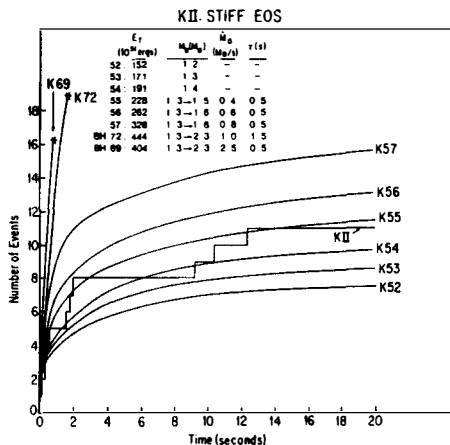


Fig. 3. Integrated number of  $\bar{\nu}_e$  events versus time in seconds expected in KII for the stiff EOS models 52-57, 69, and 72. A distance to the LMC supernova of 50 kiloparsecs has been assumed. The models represent gradually increasing amounts of accretion onto a  $1.3 M_\odot$  initial core. Included is  $E_T$ , the total energy radiated after 20 seconds. The line marked KII is the actual integral histogram of the KII data superposed for comparison with the models depicted. Models 69 and 79, terminated with an asterisk, resulted in black hole (BH) formation ( $M_B(\text{final}) \sim 2.3 M_\odot$ ).

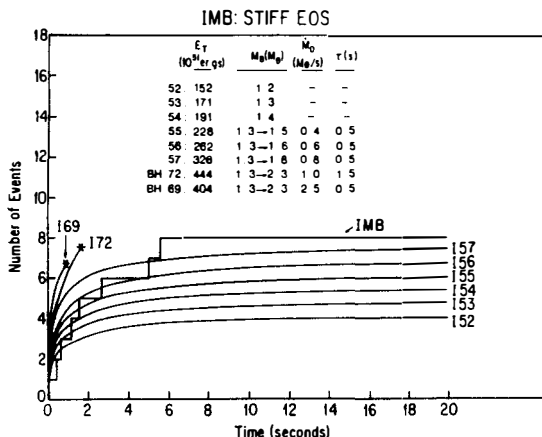


Fig. 4. Same as Figure 3, but for IMB.

and the corresponding gravitational masses are  $\sim 1.3\text{--}1.45 M_{\odot}$ . From these considerations, we can conclude that  $M_G$  of the LMC neutron star can be  $1.3\text{--}1.5 M_{\odot}$  with little difficulty. For these best-fit models, the total neutrino energy radiated after 20 seconds is  $2.0\text{--}2.5 \times 10^{53} (D/50 \text{ kpc})^2$  ergs and the total  $\nu_e$  energy radiated after 20 seconds is  $3.0\text{--}4.0 \times 10^{52} (D/50 \text{ kpc})^2$  ergs. The accretion of more than  $0.3 M_{\odot}$  onto the initial protoneutron star whose baryon mass is  $1.3 M_{\odot}$  is difficult to accommodate, as are core baryon masses as small as  $1.2 M_{\odot}$ .

## II. SN1987a-DERIVED MASS LIMIT

If the neutrino has a mass, a spectrum of energies implies a spectrum of speeds. A delta function pulse of neutrinos from SNI987a would spread as it traveled the distance between the LMC and the earth. The measured temporal spread and energy spectrum could thereby be used to obtain the neutrino mass. The delay in the neutrino arrival time with respect to the light travel time for relativistic neutrinos is easily derived to be

$$\tau = 2.57 \left( \frac{D}{50 \text{ kpc}} \right) \left( \frac{m_p}{10 \text{ eV}} \right)^2 \left( \frac{10 \text{ MeV}}{\epsilon_\nu} \right)^2 \text{ seconds} \quad , \quad (1)$$

where  $\epsilon_\nu$  is the neutrino energy and  $m_\nu$  is the neutrino mass. The distance to the LMC is approximately 50 kiloparsecs (kpc). This time is comparable to the observed temporal spread in KII and IMB. However, theory indicates that the neutrino emissions are not emitted as a sharp pulse, but over many seconds.<sup>18)</sup> Thus, the arrival time distribution in the detectors would be a convolution of the intrinsic emission distribution with the effect of a mass. That the

intrinsic emission was spread over many seconds is verified by both the KII and IMB data sets, since for no single mass do the neutrino events, with their measured energies, extrapolate back to a delta-function burst at the source.<sup>19)</sup> Indeed, the minimum possible total emission duration for the KII data is  $\sim$ 12 seconds, including all 11 events, and is  $\sim$ 2 seconds even if the last three events are dropped.

As has been emphasized,<sup>20)</sup> any mass analysis must be statistical in nature. A mass limit not in the context of an assumed source model and without an assigned probability or level of confidence is meaningless. Any mass can be made to fit the data. The question that must be asked is not whether a given mass is impossible, that can never be established, but whether that mass is suitably improbable given the data and a source model. The probability is obtained by sampling the arrival time distribution function  $N$  times, where  $N$  is the number of data points, calculating a statistic that measures the goodness-of-fit of the realization, and repeating the procedure many, many times to derive the probability distribution function (PDF) of the goodness-of-fit statistic.

The statistic is then calculated for the data points themselves, and compared to the PDF of the Monte Carlo realizations to determine what fraction of the realizations fit the model better than the data. If this fraction is 0.95, the fit is poor, and the assumed mass and source model parameters are on the 95% confidence manifold. This procedure is repeated for a wide variety of model parameters and masses to map out the parameter space and derive the entire confidence manifold. Since the dispersive effect increases as  $m_\nu^2$ , we will obtain an upper limit to  $m_\nu$ , above which the spread in the observed arrival times cannot be made to fit at a reasonable level of confidence.

The model parameter,  $f$ , is the fraction of the emissions emitted after 2.0 seconds. The source emissions were assumed to consist of an early exponential with  $\tau = 1.0$  seconds ( $t < 2.0$  seconds) and a late exponential whose time constant,  $\tau_2$ , is a function of  $f$  in such a way that the luminosity is continuous at  $t = 2.0$  seconds. Details are given in an upcoming paper by Burrows.<sup>21)</sup>

Figure 5 shows the statistically derived 25, 50, 90, 95, and 99% confidence contours in  $(m_\nu, f)$ -space. The contour segments between  $f = 0.0$  and  $f = 0.05$  are extrapolations. We see that for  $m_\nu = 0$ , there is a broad range of  $f$ 's within both the 25% and the 50% contours. As stated earlier,  $m_\nu = 0$  fits well. The most conservative upper limits to the electron neutrino mass are obtained near  $f = 0.0$ . They are 14 eV (90%), 16 eV (95%), and 19 eV (99%). The SN1987a-derived upper limits on the electron neutrino mass are more stringent than those of the SIN collaboration<sup>22)</sup> ( $<18$  eV (95%)), the LANL collaboration<sup>23)</sup> ( $<27$  eV (95%)), or the INS collaboration<sup>24)</sup> ( $<32$  eV (95%)) and are inconsistent with the 20 eV (95%) lower limit quoted by the ITEP collaboration.<sup>25)</sup> These tritium end-point experiments are being upgraded and more are being planned and tested. However, the SN1987a-derived upper limits on  $m_\nu$  are the tightest available to the physics community to date.

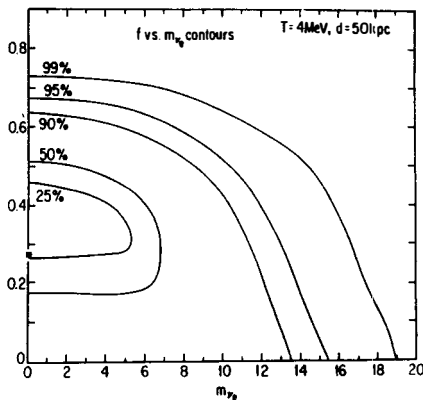


Fig. 5.  $f$  versus  $m_{\nu_e}$  confidence contours for the Monte Carlo results depicted in Fig. 7. The intersections of the  $f = 0.0$  line with the confidence contours yield the corresponding conservative mass limits. See the text for a discussion of the interpretation of the figure.

### III. CONCLUSION

What more could we hope to determine about stellar collapse and supernovae? The actual supernova mechanism still eludes us. The different mechanisms, prompt or delayed, are not unambiguously identified by only 19 events, though the smaller cores required by the prompt process are only barely allowed by the data. A Type II supernova within 10 kiloparsecs of the earth will provide 200-300 events in KII as it is now configured. Such a number should allow us to identify the shock breakout burst of  $\nu_e$ 's predicted by theory<sup>26)</sup> and intimately connected to collapse and shock phenomenology. Furthermore, though we infer that " $\nu_\mu$ 's" did indeed comprise the bulk of the emission, we did not directly detect a single one. A measurement of the neutrino flavor ratios and the  $\nu_\mu$  temperature would go a long way towards illuminating not only collapse physics, but neutrino physics as well. The SNO detector, sensitive as it is to neutral current neutrino events, is particularly relevant in this regard. Hundreds of events will allow us to constrain the neutrino masses better than we were able to with the LMC supernova. The improved statistics of proximity far outweighs the decrease in the baseline that a multitude of events would imply.

We expect, not unrealistically, that future data will answer questions we have yet to ask. Judging from the return on only 19 events,  $10^2$ - $10^3$  events should reveal a few astounding things.

## IV. REFERENCES

<sup>†</sup>This work is supported in part by the Alfred P. Sloan Foundation and by U.S. NSF Grant No. AST87-14176.

1. I. Shelton, IAU, Circular No. 4316 (1987).
2. R. M. Bionta et al., Phys. Rev. Lett. 58, 1494 (1987) (IMB Collaboration).
3. K. Hirata et al., Phys. Rev. Lett. 58, 1490 (1987) (Kamiokande II collaboration).
4. W. Baade and F. Zwicky, Phys. Rev. 45, 138 (1934).
5. D. N. Spergel, T. Piran, A. Loeb, J. Goodman, and J. N. Bahcall, Science 237 (1987), p. 1471.
6. K. Sato and H. Suzuki, Phys. Rev. Lett. 58, 2722 (1987).
7. J. Arafune and M. Fukugita, Phys. Rev. Lett. 59, 367 (1987).
8. S. A. Bludman and P. Schinder, in the proceedings of the Workshop on Extra Solar Neutrino Astronomy, UCLA, Sept. 30-Oct. 1, 1987.
9. D. N. Schramm, in the proceedings of the International Symposium on Lepton and Photon Interactions at High Energies, Hamburg W. Germany, 1987.
10. J. M. Lattimer, in Proceedings of the Minnesota conference on SNI987a, eds. T. Walsh and K. Olive, Minneapolis, Minn., June 4-6, 1987.
11. A. Burrows and J. M. Lattimer, Ap. J. (Letters) 318, L63 (1987).
12. J. van der Velde, in proceedings of the VIIth Recontre de Moriond, Les Arcs, France, Jan. 21-28, 1988.
13. J. Matthews, J., in Proceedings of the 4th George Mason Workshop in Astrophysics, ed. M. Kafatos and A. G. Michalitsianos (Cambridge University Press, Oct. 14, 1987).
14. S. W. Bruenn, Phys. Rev. Lett. 59, 938 (1987).
15. R. Mayle, J. R. Wilson, and D. Schramm, Ap. J., 318, 288 (1987) (MWS).
16. R. Mayle, in proceedings of the Minnesota Workshop on SNI987a, Minneapolis, Minn., June 5-6, 1987 (M).
17. R. Mayle and J. R. Wilson, Ap. J., in press (1987).
18. A. Burrows and J. M. Lattimer, Ap. J. 307, 178 (1986) (BL).
19. W. D. Arnett and J. L. Rosner, Phys. Rev. Lett. 58, 1906 (1987).
20. E. W. Kolb, A. Stebbins, and M. S. Turner, Phys. Rev. D, 35, 358 (1987).
21. A. Burrows, Ap. J. (Letters), May 15, in press (1988).
22. M. Fritschi et al., Phys. Lett. 173B, 485 (1986) (SIN collaboration).
23. J. F. Wilkerson et al., Phys. Rev. Lett. 58, 2023 (1987) (LANL collaboration).
24. H. Kawakami et al., in the proceedings of Telemark IV, Neutrino Masses and Neutrino Astrophysics, ed. V. Barger, F. Balzen, M. Marshak, and K. Olive (World Scientific, Singapore, 1987), p. 488, (INS collaboration).
25. S. D. Boris et al., Sov. Phys.-JETP Letters, 42, 130 (1985).
26. A. Burrows and T. J. Mazurek, Nature 301, 315 (1983).